RADIATION CHARACTERISTICS OF CYLINDRICAL DR ANTENNAS

Siu-Ming SHUM and Kwai-Man LUK
Department of Electronic Engineering, City University of Hong Kong,
83 Tat Chee Avenue, Kowloon, Hong Kong

1. Introduction

The dielectric resonator (DR) antenna is capable of providing efficient radiation up to the millimeter wave frequency band [1]. The DR antenna can be excited by penetrating a coaxial probe into its body as shown in Fig. 1. The preferred operating mode is the $HEM_{11\delta}$ mode for it produces a broadside radiation direction [1].

The radiation characteristics of the cylindrical DR antenna has been analyzed theoretically using a simple method based on a magnetic wall boundary condition [1], and using the more rigorous method of moment [2]. However, the effect of changing various parameters of the antenna on the cross-polarization level, which is important to antenna designers, has not been addressed.

In this paper, a different approach based on the finite-difference time-domain method (FDTD) is employed to undertake the analysis. Particular attention is paid to the cross-polarization properties of the antenna. The FDTD method has been applied successfully to calculating the input impedance of this type of antenna [3]. To obtain far radiation fields from the FDTD near-field data, a near-to-far field transformation process must be performed. In general, it is based on the field equivalence principle and can be performed either in the frequency domain [4] or in the time domain [5].

The frequency domain near-to-far field transformation is memory efficient: it uses a recursive Discrete Fourier Transform (DFT) algorithm, which eliminates the need for storing the whole time sequence of the fields on the virtual surface, which is mandatory in the time domain transformation. In addition, since DFT is actually more efficient than FFT when the number of observation frequencies M is smaller than $\log_2 N$, where N is the total number of time steps, the frequency domain transformation can also be more time efficient.

Here, the radiation patterns are calculated at only one or several frequencies. Therefore, the use of frequency domain near-to-far field transformation is highly efficient. Furthermore, an efficient recursive algorithm, the Goertzel Algorithm [6] for DFT calculation is used, which further speeds up the analysis process.

2. Analysis Method

According to the field equivalence principle, the electromagnetic fields outside an imaginary closed surface surrounding the object of interest can be obtained if the tangential fields on the closed surface is known. Consequently, In the FDTD simulation, the time domain fields on a surface enclosing the DR antenna is used to calculate the far radiation fields. The time domain fields are converted to the frequency domain using an efficient recursive algorithm called the Goertzel Algorithm. The DFT is considered as a linear filtering operation with the following system function [6]

$$H_k(z) = \frac{1}{1 - W_N^{-k} z^{-1}} \tag{1}$$

where z is the z-transform variables. After manipulating $H_k(z)$, two difference equations can be obtained for calculating the DFT of a time sequence F(n):

$$v_k(n) = 2\cos\left(\frac{2\pi k}{N}\right) v_k(n-1) - v_k(n-2) + F(n) \tag{2}$$

$$y_k(n) = v_k(n) - W_N^k v(n-1) \quad (3)$$

where $W_N^k = \cos(2\pi k / N) - j\sin(2\pi k / N)$. The recursive relations in (2) is iterated for n = 0,1,...,N but equation (3) is computed only once at a time n = N, which yields the component of F(t) at frequency f_k. = 1/NkΔt, where N is the total number of time steps and Δt is the time step. Hence, in each FDTD time step and each frequency of interest, only one real multiplication and two additions are required for each tangential field component on the closed surface chosen for far fields calculation. This is more efficient than the conventional recursive DFT method which requires two real multiplications and two additions.

Once the frequency domain near fields on the virtual surface are available at the end of the FDTD simulation, these fields are integrated with the free-space Green's function weighting to obtain the far fields.

3. Results

The DR antenna first considered has parameters: ε_r = 9.2, a = 6.1 mm, b = 4.15 cm, d = 12.2 mm and l = 5.1 mm. The far fields of the DR antenna are obtained from the FDTD data using the mentioned technique. The radiation patterns of the fabricated antenna are measured in an anechoic chamber using a HP85310C Antenna Measurement System. Both the calculated and the measured radiation patterns are shown in Fig. 2. The agreement between both results is quiet good. The discrepancies are mainly due to the infinite ground plane assumption used in the calculation.

Next, the effect of changing the probe position on the radiation patterns of the antenna is investigated. The dimensions of the antenna is unchanged and the distance of the probe from the center of the DR, b is varied between 0.2 a and 0.9 a. For each value of b, the probe length is adjusted to maintain impedance matching. The results on radiation patterns for three different values of b/a are plotted in Fig. 3a to Fig. 3c. In addition, The E-Plane and the H-Plane cross-polarization are plotted against b/a in Fig. 4. From these figures, it can be seen that as b is increased, both the cross-polarization level and the asymmetry of the E-Plane pattern is reduced. Hence, the feeding probe should be located as close to the edge of the DR as possible. It is worth noting that the resonant frequency of the antenna only changes slightly when the probe position is changed.

The effect of changing the ratio of the radius and the height of the DR is also studied. The radiation patterns for three different values of a/d are plotted in Fig. 3d to Fig. 3f. The E-Plane and the H-Plane cross-polarization are plotted against a/d in Fig. 5. Again, for each value of a/d, the probe length is adjusted to maintain impedance matching. From these figures, it is observed that small values of a/d produces smaller cross-polarized fields. However, if a/d is smaller than 2.0, it may be different to match the input impedance of the antenna to 50 Ω. Since a is fixed, the resonant frequency increases when a/d is increased.

Finally, the cross-polarization of the DR antenna is considered as a function of the angle ϕ. The calculated results are plotted in Fig. 6. As shown in the figure, the cross-polarization level attains a maximum at ϕ = 45° and ϕ = 135°.

Conclusion

An efficient FDTD with frequency domain near-to-far field transformation is used to obtain the far fields of the cylindrical DR antenna. The calculated results are consistent with measured results. It is found that, to achieve a low polarization level, the feeding probe should be located near to the edge of the DR and the ratio of the radius and the height of the DR antenna should be kept small.

Acknowledgment

This project are supported by a UGC Earmarked Grant of Hong Kong and a CITYU Strategic Research Grant.

References

1. LONG, S. A., MCALLISTER, M. W., and SHEEN, C.: 'The resonant cylindrical dielectric cavity antenna', *IEEE Trans. Antennas and Propagation*, 1983, vol. 31, pp. 406-412
2. KISHK, A. A., AUDA, H. A. and AHN, B. C.: 'Radiation characteristics of cylindrical dielectric resonator antennas with new applications', *IEEE Antennas and Propagation Society News Letter*, 1989, vol. 31, pp. 7-16
3. SHUM, S. M., and LUK, K. M.: 'FDTD analysis of probe-fed cylindrical dielectric resonator antenna operating in fundamental broadside', *Electron. Lett.*, 1995, vol. 31, pp. 1210-1212
4. TAFLOVE, A., and UMASHANKAR, K. R.: 'Radar cross section of general three-dimensional structures', Electromagnetic Compatibility, 1983, vol. 25, pp. 433-440
5. LUEBBERS, R., J., KUNZ, K. S., SCHNEIDER, M. and HUNSBERGER, F.:'A finite-difference time-domain near zone to far zone transformation', *IEEE Trans. Antennas and Propagation*,1991, vol. 39, pp. 429-433
6. OPPENHEIM, A. V. and SCHAFER, R. W.: *Discrete-time signal processing*, Prentice Hall, Chap. 9, pp. 585-587

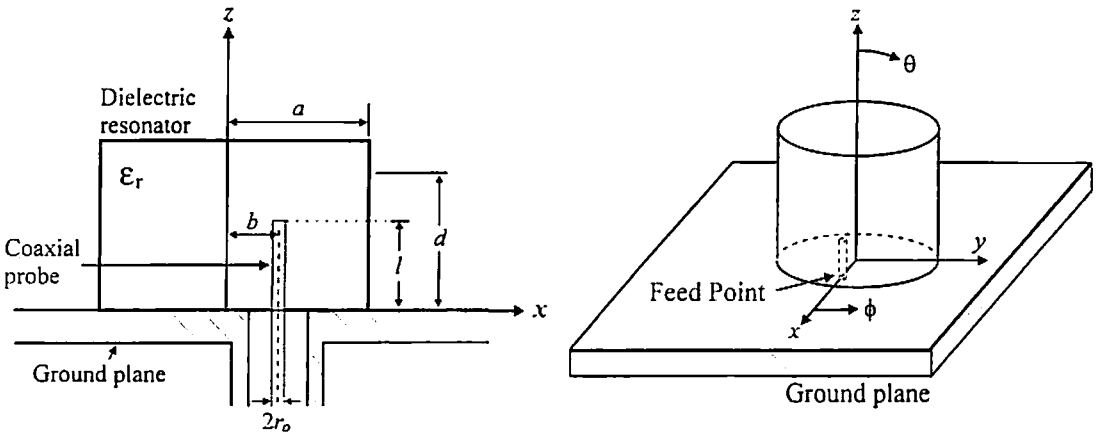

Fig. 1. The geometry of the probe fed cylindrical DR antenna

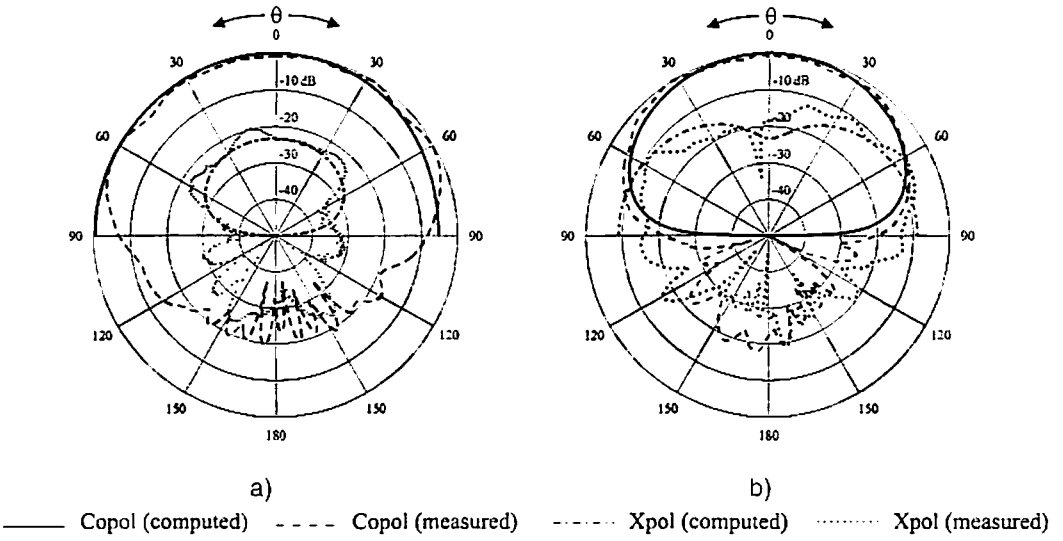

Fig. 2. Calculated and measured radiation patterns (a) E-Plane (b) H-Plane

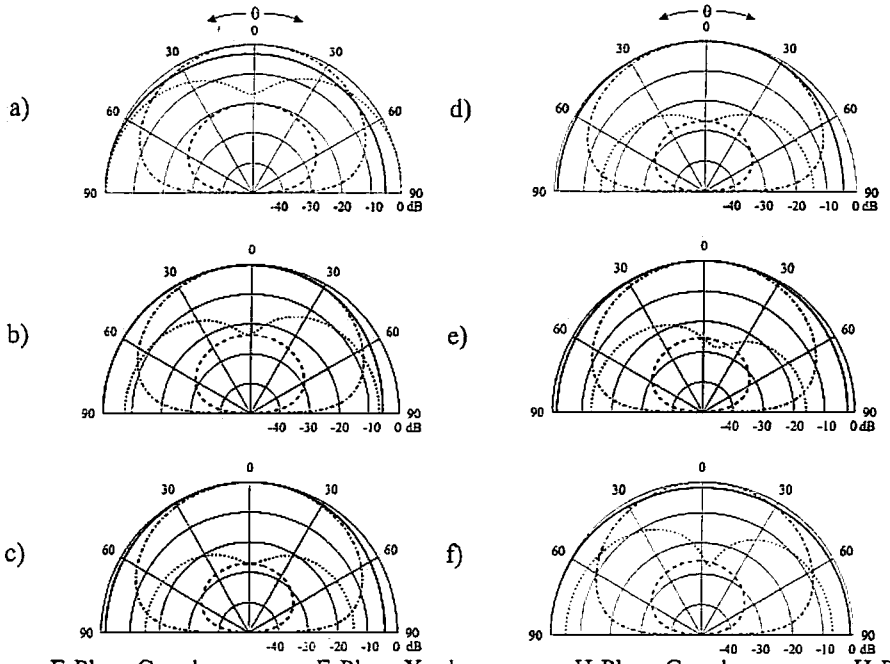

E-Plane Copol - - - - - E-Plane Xpol -·-·-·- H-Plane Copol ····· H-Plane Xpol

Fig.3 Far field patterns for different b/a and a/d.
a) b/a = 0.3, b) b/a = 0.6, c) b/a = 0.9, d) a/d = 0.4, e) a/d = 1.0 & f) a/d = 1.6

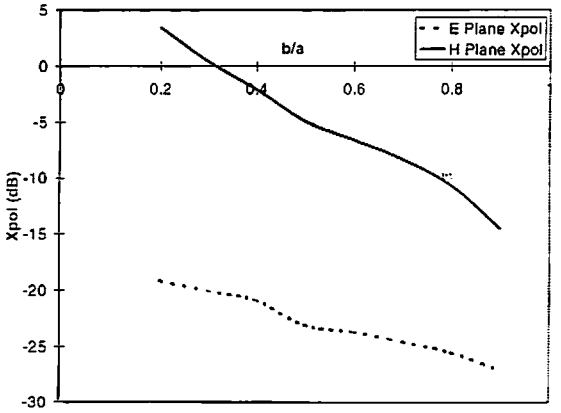

Fig. 4. Cross-polarization level versus b/a

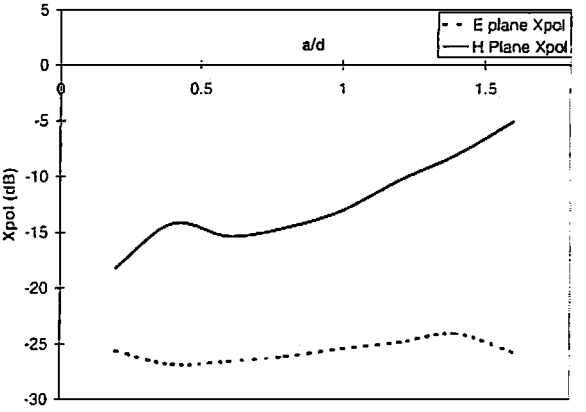

Fig. 5. Cross-polarization level versus a/d

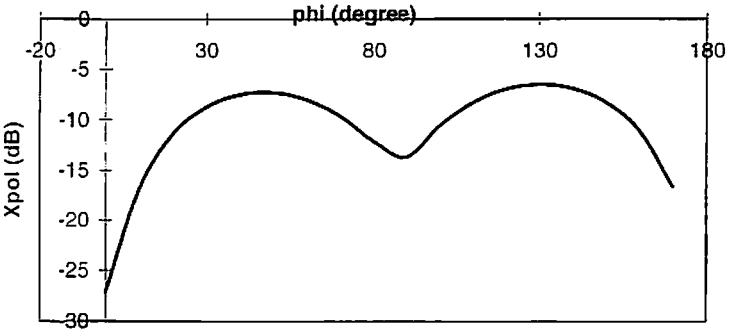

Fig. 6. Cross-polarization versus angle ϕ